PhotoniX Life

Open Access
PhotoniX Life (2026)1:12
https://doi.org/10.3724/PXLIFE.2025-0005

Review

Cell segmentation in live-cell microscopy with deep learning

Zhijun Tan[1#], Yang Ding[1#], Jintao Li[1], Bin Fang[2], Hua Bai[1*], Bo Peng[1*] AND Lin Li[1,2*]

[1]State Key Laboratory of Flexible Electronics (LoFE) & Institute of Flexible Electronics (IFE), Northwestern Polytechnical University, Xi'an 710072, China;
[2]State Key Laboratory of Flexible Electronics (LoFE) & Institute of Flexible Electronics (IFE, Future Technologies), Xiamen University, Xiamen 361102, China

* Corresponding authors (emails: iamhbai@nwpu.edu.cn (H.B.); iambpeng@nwpu.edu.cn (B.P.); iamlli@nwpu.edu.cn (L.L.))
# These authors contributed equally to this work

Received 8 April 2025; accepted 23 September 2025; published online 15 June 2026

Abstract Live-cell imaging plays a pivotal role in revealing cellular morphology and dynamics, providing critical insights into fundamental biological mechanisms and disease pathogenesis. Image segmentation techniques hold great promise for enabling the quantitative analysis of cellular features, measuring morphological phenomena at the single-cell level. Although traditional segmentation methods are computationally efficient, they often struggle with complex biological data. Advances in deep learning underpin a collection of algorithms with an impressive ability to interpret image content, providing new perspectives on challenges such as cellular heterogeneity, diverse imaging modalities, and real-time analysis in live-cell segmentation. Looking ahead, we discuss key directions that include improving model generalizability across biological systems, advancing three-dimensional volumetric segmentation, and prioritizing user-friendly design. These advancements have deepened our understanding of pathology and facilitated the development of therapeutic strategies, emphasizing the transformative impact of computational innovation on biomedical research and diagnostics.

Keywords image segmentation, live-cell imaging, artificial intellegence, deep learning

1. Introduction

Cells, as the fundamental units of life, carry out the complex processes essential for sustaining organisms [1,2]. Studying their morphology and dynamic behaviors provides a critical window into understanding biological mechanisms [3]. By elucidating how cells function, interact, and respond to various stimuli, researchers gain valuable insights into biological systems and develop a strong foundation for medical interventions [4]. To achieve this, it is crucial to visualize and analyze cellular morphology and behaviors with high precision [5,6]. Advanced microscopy techniques now enable scientists to observe cellular morphology and real-time activities at submicron resolutions, even revealing pathological changes invisible to conventional methods [7,8]. When combined with computational tools, these imaging datasets transform into rich biological insights, broadening our understanding of cellular function and fostering innovations in biomedical science [9,10].

Live-cell imaging revolutionizes how we study living systems by capturing real-time visualization of unperturbed cellular dynamics [11]. Fluorescent probes allow longitudinal tracking of these events with low phototoxicity, producing rich spatiotemporal datasets that chronicle cellular life [12-14]. Yet this wealth of information presents a formidable analytical frontier [15]. The inherent complexity of live-cell datasets, characterized by low signal-to-noise ratios (SNR), temporal variability, and structural heterogeneity, demands robust computational tools to accurately delineate cell boundaries and parse overlapping structures [16,17].

Traditional image segmentation methods, such as thresholding and watershed algorithms, offer simplicity and efficiency, but their mechanistic rigidity becomes apparent in live-cell scenarios [18]. Thresholding relies on intensity values to separate foreground and background, yet it is extremely sensitive to uneven illumination and temporal fluctuations (Figure 1a) [19]. The watershed algorithm, which treats image gradients as topographic surfaces, often suffers from over-segmentation nightmares when applied to confluent cell populations (Figure 1b) [20]. More critically, these approaches require extensive manual parameter tuning and lack generalizability across diverse imaging modalities, limiting their utility in live-cell studies where precision and adaptability are paramount [21]. Furthermore, when applied to three-dimensional (3D) images, traditional segmentation methods struggle with increased data volume, anisotropic resolution, and especially the challenge of modeling spatial continuity across slices [22]. Manual thresholding and parameter tuning are often insufficient, resulting in fragmented and inaccurate segmentations that limit their use for volumetric cell analysis.

Deep learning leverages hierarchical feature extraction and learning to demonstrate remarkable capability in decoding biological complexity, fundamentally transforming cellular image analysis [21,23,24]. At the heart of this revolution are convolutional neural networks (CNNs) that emulate expert visual cognition, enabling precise delineation of cellular boundaries even in densely packed or low-contrast environments [25,26]. By

© The Author(s) 2026. This is an Open Access article distributed under the CC BY-NC-ND license (https://creativecommons.org/licenses/by-nc-nd/4.0/).

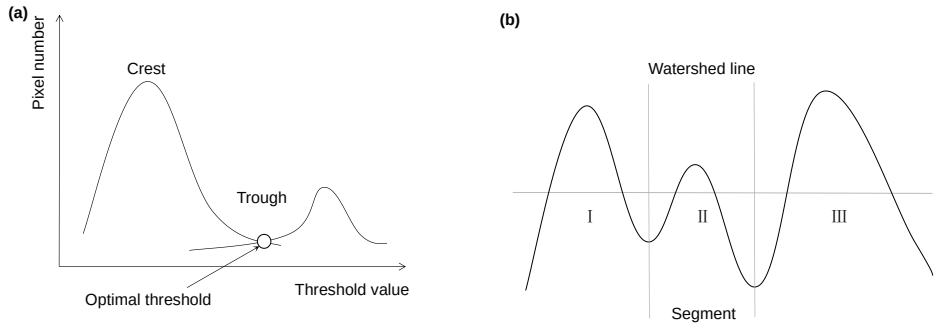


Figure 1 The principles of traditional segmentation methods. **a.** The principles of threshold for image segmentation; **b.** the principles of watershed methods for image segmentation.

integrating temporal context and multi-scale features, deep learning models bridge the gap between high-resolution imaging and automated analysis pipelines, facilitating tasks such as real-time tracking, morphological quantification, and anomaly detection [27]. This synergy between imaging and computation is redefining the scalability and reproducibility of live-cell studies, empowering researchers to interrogate biological systems at unprecedented spatiotemporal resolution [10,28]. Meanwhile, deep-learning approaches enhance 3D segmentation performance by effectively modeling spatial complexity and learning hierarchical features across all three axes, enabling accurate and robust segmentation in complex volumetric datasets [29,30].

In this review, we focus on the advancements in deep learning combined with image segmentation for live-cell microscopy, emphasizing their transformative impact on biomedical research. We first introduce the foundational principles, methodologies, and evaluation standards of image segmentation techniques, emphasizing their role in decoding cellular morphology and dynamics. We then highlight their transformative applications across cellular systems, including single-cell tracking in eukaryotic cells. Critical challenges such as model generalizability, 3D volumetric segmentation, and user-friendly design are analyzed, with emerging solutions emphasizing self-supervised learning, interactive frameworks, and automated pipelines.

2. Image segmentation

2.1 Principles of image segmentation

Traditional image segmentation relies on rule-based algorithms that delineate regions using features such as intensity, edges, or spatial homogeneity [31]. Deep learning has fundamentally transformed segmentation by establishing end-to-end frameworks capable of learning hierarchical feature representations directly from raw data, overcoming the inherent limitations of classical algorithms [32,33]. Its core principle lies in optimizing pixel-wise classification through supervised learning, where neural networks automatically extract and integrate multi-level spatial features to generate dense, structured predictions [34,35]. CNNs form the bedrock of this transformation, excelling at capturing multi-scale spatial patterns from local textures to global contexts, enabling precise cellular boundary delineation even in low-contrast or noisy environments (Figure 2a) [25].

2.2 Existing methods

Traditional methods prioritize computational simplicity but require laborious manual adjustments to adapt to diverse biological scenarios [19,20,36,37]. Improved traditional approaches, such as active contour models and adaptive thresholding, offer enhanced flexibility and robustness for segmenting tissues and cells with irregular shapes or non-uniform intensities. However, they still require careful parameter selection and often lack generalizability in complex imaging scenarios [38-40].

Deep learning-based segmentation began with fully convolutional networks (FCNs), which replaced fully connected layers with dynamic convolutional operations, preserving spatial resolution for pixel-wise predictions (Figure 2b) [41]. This innovation catalyzed specialized architectures like U-Net, its encoder-decoder symmetry, and skip connections, which act as computational synapses, achieving high-precision segmentation even with limited training data (Figure 2c) [42]. When confronting densely packed cells, Mask R-CNN's dual-stream design tackles the challenge: its region proposal network (RPN) scouts different cells while parallel mask branches refine boundaries (Figure 2d) [43]. ResNet introduces residual blocks and uses skip connections to solve the vanishing gradient problem in deep networks (Figure 2e) [44]. These models transcend traditional methods by autonomously adapting to dynamic biological data, quantifying morphological parameters, and providing scalable, data-driven insights into cellular behaviors and disease mechanisms. Their synergy of accuracy, generalizability, and multi-task integration establishes deep learning as the cornerstone of live-cell imaging segmentation (Table 1) [45-48].

2.3 Evaluation metrics

Evaluating segmentation accuracy demands a tripartite approach: regional congruence, boundary precision, and pixel-level metrics [49]. The Dice coefficient clearly exposes under-segmented regions, while the stricter boundary sensitivity of intersection over union (IoU) penalizes jagged cell edges (Figure 3). For high-resolution image analysis, the Harsdorff distance serves as a stringent boundary measure, quantifying even micron-level deviations between predicted and true boundaries. Average surface distance (ASD) operates as the meticulous cartographer, mapping systemic alignment errors across entire cell populations. Among pixel-level metrics, the F1-score balances precision and

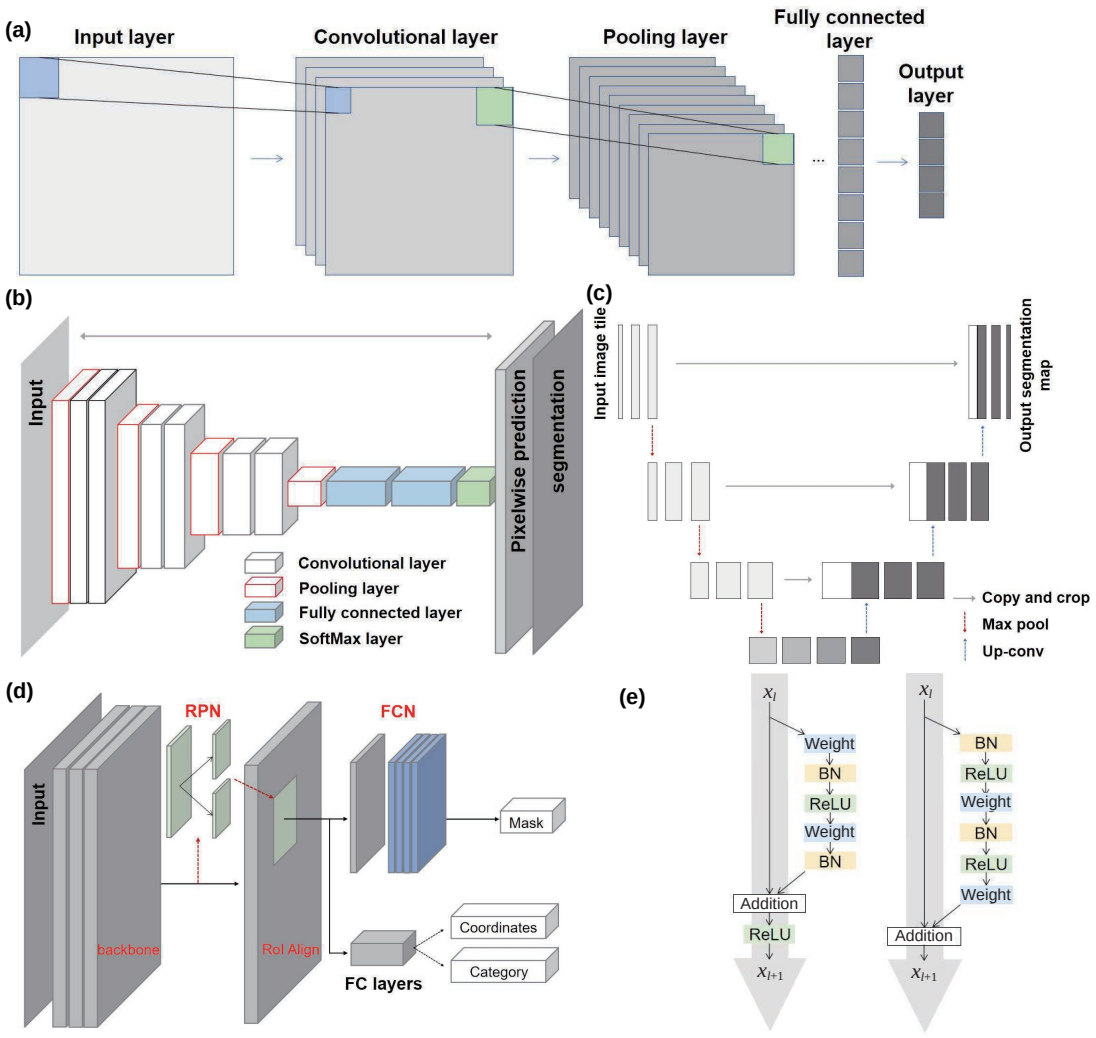


Figure 2 The principles of deep learning methods. **a.** The principles of CNNs for image analysis are shown, including convolutional operations, pooling, and fully connected layers; **b.** U-Net uses skip connections between the max pooling and the up-sampling, improving feature extraction and localization; **c.** the FCN employs forward inference and backward learning, transforming input images into segmented outputs; **d.** Mask R-CNN architecture combining RPN with fully connected layers to predict masks, classes, and bounding boxes simultaneously for each object in an image; **e.** residual network (ResNet) introduces residual blocks and skip connections, enabling the network to learn residuals between inputs and outputs. This alleviates issues of vanishing or exploding gradients and network degradation. The left side is the original structure, and the right side is the optimized structure. BN: batch normalization; ReLU: rectified linear unit.

recall, ideal for small or sparsely distributed targets [50,51]. Standardized evaluation protocols and visual validation are indispensable, particularly for cell tracking and morphological analysis, which demands high recall to avoid missed detections and prioritizes high Dice coefficients to ensure regional integrity [52]. Current bottlenecks manifest in paradoxical form: while 3D+t datasets balloon into terabyte-scale dimensions, the gold standard remains almost pathologist-drawn contours on two-dimensional (2D) slices. This mismatch is driving innovations like virtual labeling through physics-informed generative adversarial network (GANs) and self-supervised learning, reducing reliance on large-scale annotated datasets [53].

In summary, image segmentation has evolved from feature-based methods to deep learning-driven methods, progressively addressing challenges such as noise, overlap, and dynamic variations in biomedical imaging. The adaptability of deep learning has established it as the cornerstone of live-cell imaging analysis, while diversified evaluation metrics provide scientific guidelines for algorithmic optimization [54,55].

3. Cell image segmentation

Cell image segmentation is one of the foundational tasks in biomedical imaging, supporting the analysis of cellular morphology, function, and interactions. By accurately delineating the boundaries of cells in microscopy images, segmentation enables downstream tasks such as cell counting, tracking, and morphological classification, which are crucial for understanding biological processes and disease mechanisms (Table 2) [56-70]. However, the significant variability in cell shapes, sizes, and imaging conditions poses substantial challenges, necessitating advanced computational approaches to achieve accuracy and

Table 1 Comparison of traditional and deep learning-based image segmentation methods

Category	Method	Key features	Strengths	Limitations
Traditional	Thresholding [19]	Pixel intensity thresholding	Simple and fast	Fails under uneven illumination
	Watershed [20]	Region-based	Effective in separated structures	Over-segmentation in dense regions
	Active contour [38] Adaptive thresholding [39]	Flexible for irregular shapes; needs manual tuning	Improved adaptability for variable shapes	Requires careful parameter tuning
Deep learning	FCNs [41]	Replaces fully connected (FC) layers with conv layers; supports dense prediction	Preserves spatial resolution; generalizable	Needs labeled training data
	U-Net [42]	Encoder-decoder structure; skip connections enhance localization	High precision; works well with limited data	May struggle with very complex instances
	Mask R-CNN [43]	Region proposals + instance masks; good for overlapping cells	Handles instance-level detection	High computational cost
	ResNet [44]	Residual blocks mitigate vanishing gradients	Deep architecture; robust feature learning	Primarily used as a feature extractor
	ViT [45] Swin transformer [46]	Attention mechanism; captures long-range dependencies	Scalable; good at modeling context	Data hungry; needs large-scale training
	Segment anything model (SAM) [47,48]	Prompt-driven, general-purpose segmentation	Zero-shot capability; flexible across domains	Still under optimization for biological data

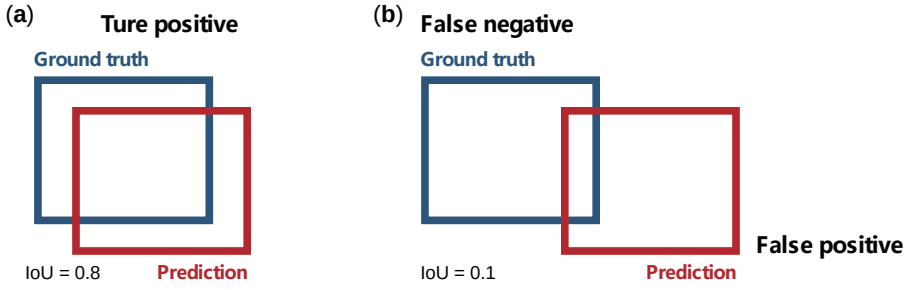


Figure 3 Evaluation metrics for image segmentation performance. **a.** The predicted segmentation (red box) overlaps significantly with the ground truth (blue box), achieving an IoU value of 0.8, which indicates a high-quality match. **b.** In the false negative scenario, the prediction (red box) fails to overlap adequately with the ground truth (blue box), resulting in an IoU of 0.1. Additionally, the red box illustrates a false positive, where the predicted area does not correspond to a valid ground truth region.

scalability [32].

Cell segmentation originated in the mid-20th century, initially relying on manual tracing of cellular boundaries. Manual tracing proved inefficient for handling the data volumes generated by high-throughput screening, driving the development of automated methods. Early automated approaches adopted classical image processing techniques. In 2006, Chen et al. [56] proposed using Otsu's thresholding method to segment cell nuclei, enabling the classification and tracking of tumor cells in time-series fluorescence microscopy images. Although effective for high-contrast images, this method struggled with uneven illumination and overlapping targets. The watershed algorithm, which interprets intensity maps as topographical landscapes to separate adjacent cells, was also widely adopted [71]. While powerful, it often resulted in over-segmentation in noisy or densely packed images. In 2015, Ji et al. [57] proposed a distance transform-based watershed algorithm to address issues of cell adhesion in images, effectively mitigating cell adhesion and over-segmentation problems. Despite its innovative design, this method required precise initialization and was highly sensitive to noise. To improve performance, in 2019, Abdolhoseini et al. [58] developed a hybrid framework combining locally adaptive thresholding, effectively addressing the problem of heavily clustered nuclei. Niaz et al. [59] introduced a self-initialized active contour model, which eliminates the need for contour initialization. Fang et al. [60] proposed a multi-scale histogram thresholding technique, employing ellipse fitting to better segment overlapping or variably shaped cells.

The limitations of these approaches, such as the need for extensive manual tuning and lack of generalizability, particularly when applied to diverse datasets, drove the adoption of deep learning methods, which offered automatic feature extraction and improved generalization. One of the earliest successes in this transition was the introduction of the U-Net by Ronneberger et al. [61] in 2015. U-Net combined an encoder-decoder architecture with skip connections, achieving exceptional segmentation accuracy in biomedical images. U-Net was originally developed and evaluated on datasets from serial section transmission electron microscopy, phase contrast microscopy, and DIC microscopy. While highly effective for small, annotated datasets, the U-Net's performance declined when applied to diverse cell types and imaging modalities, highlighting the need for models with enhanced generalization capabilities.

To address this, researchers developed more robust and versatile

Table 2 Summary of representative algorithms and techniques for cell and nucleus image segmentation

Category	Algorithm	Technique	Application	Modality	Accuracy	Speed	3D capable	User-friendliness	Dataset details
Traditional	Chen et al. [56]	Otsu's thresholding and K-nearest neighbor (KNN) classification	Segmentation, tracking, and phase identification	Fluorescence microscopy	–	–	No	–	16 sample images (~3,071 nuclei)
	Ji et al. [57]	Watershed enhanced by distance transformation	Adherent cell segmentation	Light microscopy images	–	–	No	–	No specific dataset
	Abdolhoseini et al. [58]	Locally adaptive thresholding	Breast cancer H&E tissue, neuron tissue	Fluorescence microscopy	F1 = 0.88, IoU = 0.78	1 s/400 pixels × 400 pixels (CPU)	Yes	–	16 images, ~400 pixels × 400 pixels
	Niaz et al. [59]	Self-initializing level-set active contour	–	Brightfield & phase-contrast microscopy	Dice = 0.96, IoU = 0.92	–	No	–	Public nuclei image dataset
	Fang et al. [60]	Multi-scale histogram thresholding	–	Fluorescence microscopy	IoU = 0.94	–	No	Implemented in MATLAB	NIH3T3 dataset
Deep learning	Ronneberger et al. [61]	U-Net	Segmentation and tracking	Transmission election microscopy (TEM)	IoU = 0.92	1 s/512 pixels × 512 pixels (GPU)	No	ImageJ	SBI Cell Tracking challenge
	StarDist 1.0 [62]	U-Net and non-maximum suppression (NMS)	Nuclei and cell segmentation	Fluorescence microscopy	AP@0.5 = 0.86	0.5 s/512 pixels × 512 pixels (GPU)	No	Fiji	2018 Data Science Bowl training set
	StarDist 2.0 [63]	ResNet and NMS	3D nuclei segmentation	Fluorescence microscopy	IoU = 0.93	9 s/1, 141 pixels × 140 pixels × 140 pixels (GPU)	Yes	Python integrations	WORM and PARHYALE
	2018 Data Science Bowl [64]	U-Nets, FPNs, and Mask-RCNN	Spanning over 30 biological experiments	Fluorescence microscopy	F1 = 0.71, IoU = 0.77	–	No	Pretrained model	BBBC038
	Falk et al. [65]	U-Net, advanced morphometric version	Detection and segmentation	Fluorescence, bright-field, differential interference contrast (DIC), electron microscopy (EM)	–	–	Yes	Fiji/ImageJ plugin, GUI	SBI Cell Tracking Challenge 2015
	Cellpose 1.0 [66]	Modified U-Net with style transfer, vector flow representation	General cell/nuclear types	Fluorescence, bright-field microscopy	AP@0.5 = 0.94	0.30 s/ 512 pixels × 512 pixels (GPU)	Yes	GUI, Python API	608 images, >70,000 cells
	Cellpose 2.0 [67]	Human-in-the-loop and "model zoo"	Retrained on TissueNet and LiveCell	Fluorescence, phase contrast microscopy	AP@0.5 = 0.90	–	Yes	GUI	Cellpose, TissueNet, LiveCell
	Cellpose 3.0 [68]	Denoising and deblurring using perceptual and loss functions	General whole-cell/nuclear types	Widefield/ confocal microscopy	AP@0.5 = 0.92	–	Yes	GUI	Cellpose cyto2, TissueNet, LiveCell
	Mesmer [69]	ResNet50 and feature pyramid network (FPN)	General whole-cell/nuclear types	General-purpose imaging modality	F1 = 0.88	13 s/512 images × 512 images (GPU)	No	GUI	TissueNet
	SCS [70]	Transformer neural network	Spatial transcriptomics, metabolic flux	2D tissue slices	Dice = 0.88, IoU = 0.70	0.32 s/512 pixels × 512 pixels (GPU)	No	Pretrained model	STARmap, Stereo-seq

architectures. In 2018, Schmidt et al. [62] introduced StarDist 1.0, a groundbreaking model for cell and nucleus segmentation that utilized star-convex polygons to accurately delineate cell shapes in crowded and irregular microscopy images. StarDist was benchmarked using diverse fluorescence microscopy images of cell nuclei, particularly those from the Data Science Bowl 2018 dataset. Unlike traditional bounding box-based methods, StarDist predicted radial distances from each pixel to the object boundary in 32 directions, enabling flexible, high-fidelity shape representations. Built on a U-Net backbone, the architecture produced object probabilities and polygon parameters, resolving overlaps through NMS. This approach minimized errors such as merging adjacent nuclei and outperformed previous algorithms on both synthetic and real-world datasets (Figure 4a and b). Expanding on this, StarDist 2.0 extended the concept to volumetric fluorescence microscopy in 2020 [63]. StarDist2.0 was evaluated on volumetric fluorescence microscopy datasets, including DAPI- and EGFP-labeled nuclei from *C. elegans* and *Parhyale* hawaiensis embryos. By predicting star-convex polyhedra, it addressed challenges in 3D shape representation and anisotropic voxel sizes. Using a ResNet backbone and efficient intersection calculations, it balanced precision and computational efficiency, outperforming 3D U-Net and traditional segmentation techniques on low SNR datasets (Figure 4c and d). These innovations establish StarDist as a robust tool for cell segmentation in both 2D and 3D imaging.

Following the advancements in handling complex and crowded cell segmentation, subsequent studies addressed challenges such as cross-modal generalizability and usability across diverse imaging systems. A pivotal development came with the 2019 Data Science Bowl, which promoted the creation of models capable of segmenting nuclei across various imaging modalities and experimental conditions without requiring manual configuration [64]. These models employed ensemble approaches and FPN to outperform classical algorithms. By training on a diverse dataset comprising over 37,000 annotated nuclei from 30 different experiments, the top-performing solutions demonstrated robust generalization on unseen datasets, setting a benchmark for configuration-free segmentation tools. Additionally, the U-Net architecture was extended in 2019 to offer adaptable pipelines for new tasks with minimal annotated data [65]. This extension prioritized usability, incorporating a user-friendly plugin integrated with ImageJ, thereby making deep learning tools accessible to non-experts. These innovations paved the way for bridging the gap between task-specific models and general-purpose solutions in image segmentation.

Cellpose represents a milestone in the development of generalist models for cellular segmentation, addressing the limitations of earlier specialized approaches [66-68]. Introduced in 2021, Cellpose 1.0 was built on a modified U-Net architecture that predicted spatial gradients and binary masks to identify cell boundaries [66]. The distinct feature was its gradient tracking algorithm, which allowed grouping of pixels based on flow convergence, enabling accurate segmentation of cells with diverse shapes. Trained on a comprehensive dataset of over 70,000 cell instances spanning various imaging modalities and cell types, the model demonstrated high adaptability without requiring additional fine-tuning. Furthermore, Cellpose 1.0 included a graphical user interface (GUI), making it accessible to users without deep learning expertise (Figure 5a). Building on this foundation, Cellpose 2.0, introduced in 2022, addressed the challenge of customizing models for specific use cases [67]. Cellpose 2.0 includes models trained and evaluated on images from fluorescence, phase-contrast, and brightfield, across various tissue types and cell lines. It featured a human-in-the-loop pipeline, allowing users to fine-tune pretrained models with as few as 100–200 annotated region of interest (ROI) (Figure 5b). This version also introduced "model zoo", an ensemble of models trained on distinct segmentation styles, which automatically selected models tailored to the user's dataset (Figure 5c). This

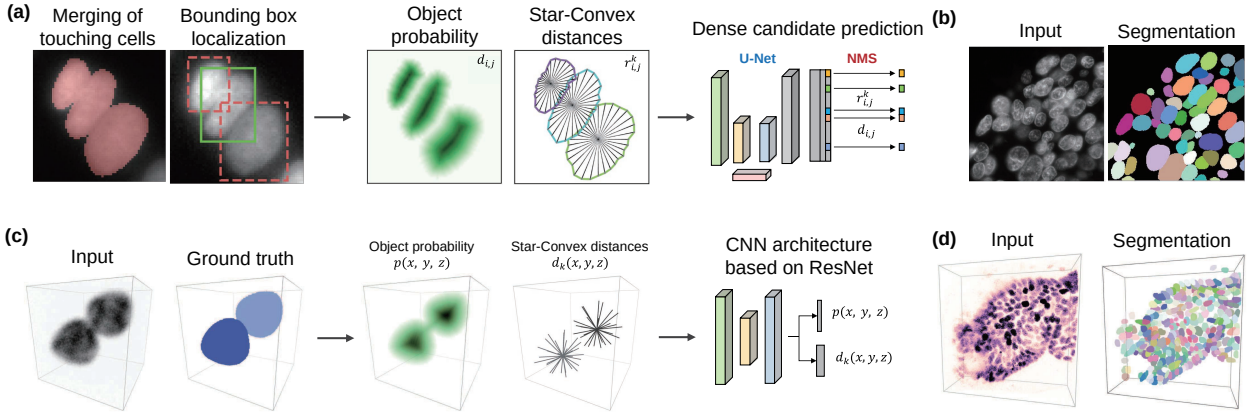


Figure 4 StarDist 1.0 and 2.0 for addressing segmentation challenges in 2D and 3D images with crowded nuclei. **a.** Segmentation errors may arise due to the merging of touching cells or suppression of valid cell instances caused by large overlaps in bounding box localization. The StarDist 1.0 addresses these issues by predicting both object probabilities and star-convex polygons, parameterized by radial distances. The method employs a U-Net architecture to densely predict object properties and radial distances, followed by NMS to select the final instances. **b.** The 2D segmentation results of the StarDist 1.0 method, showing precise identification and separation of nuclei. **c.** StarDist 2.0 is trained to densely predict object probabilities and radial distances to object boundaries in a 3D image. The CNN architecture used in StarDist 2.0 is based on ResNet, enabling robust feature extraction and prediction for 3D data. **d.** The 3D segmentation results of the StarDist 2.0 method.

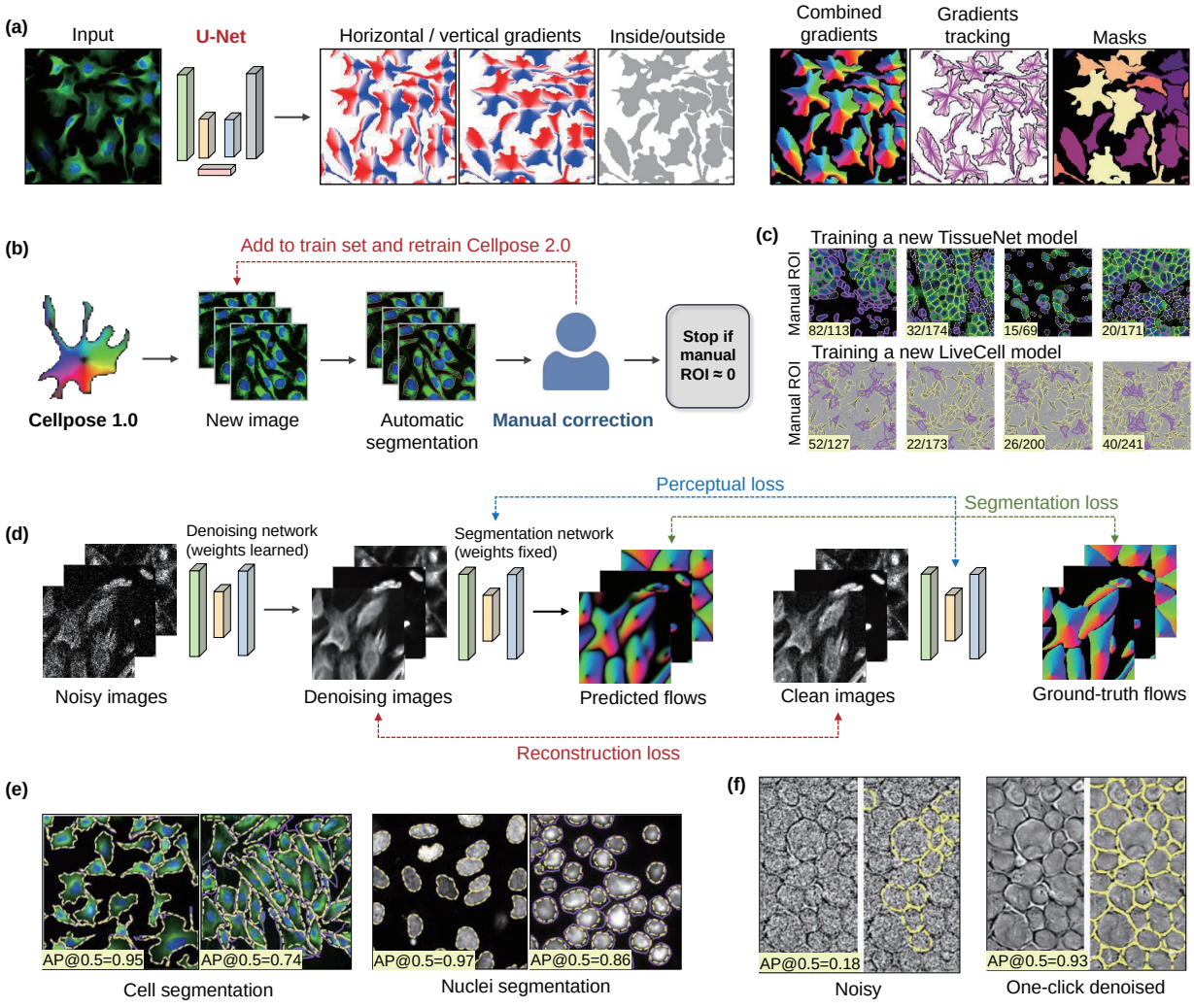


Figure 5 Overview of Cellpose 1.0−3.0 for cell segmentation and denoising. **a.** Cellpose 1.0 segmentation pipeline, the neural network predicts horizontal and vertical gradients and cell pixel probabilities, combining them into a gradient vector field. Using a U-Net backbone with skip connections and global style features, the network generates fixed points whose basins of attraction correspond to cell masks. In inference, pixels are dynamically grouped into masks based on gradient convergence. **b.** Human-in-the-loop workflow in Cellpose 2.0, the iterative annotation process allows human correction of missed or mis-segmented regions, followed by model retraining. Yellow outlines denote correctly identified cells, while purple outlines show newly added cells by human annotation. This approach ensures continuous improvement of model performance. **c.** After the TissueNet and LiveCell model retraining step, the updated model was applied to the next image, with human curators correcting segmentation errors. The workflow ensures accurate segmentation with minimal manual intervention. **d.** Cellpose 3.0 integrates segmentation and denoising with a protocol combining perceptual, reconstruction, and segmentation losses, leveraging high-resolution training data to enhance segmentation quality and reduce noise in complex images. **e**. Segmentation performance on cell and nuclei datasets. The AP@0.5 is the AP of the segmentation at an IoU threshold of 0.5. **f**. One-click model for denoising. After using the one-click model (right), good denoising effects were achieved, realizing accurate cell segmentation. AP@0.5 reported.

innovation bridged the gap between generalization and specificity, achieving performance levels comparable to models trained on tens of thousands of annotated images.

Further advancing the framework, Cellpose 3.0, proposed very recently, incorporated a novel image restoration module to address challenges like noise and blurriness [68]. Cellpose 3.0 was trained on cellular and non-cellular images, including confocal, widefield fluorescence, two-photon, and brightfield imaging microscopy modalities, emphasizing robustness to noise, blur, and undersampling across platforms. Unlike traditional denoising methods that optimize pixel-level reconstruction, Cellpose 3.0 trained restoration networks to enhance segmentation quality directly. By coupling perceptual and segmentation losses, it restored image fidelity while improving segmentation accuracy on cell and nuclei datasets (Figure 5d and e). This version also seamlessly integrated into the GUI, offering a one-click restoration option for noisy or undersampled images, expanding its usability in experimental settings (Figure 5f). The iterative development of Cellpose demonstrates a roadmap for addressing complex segmentation challenges, setting a new benchmark for scalable and user-friendly segmentation technologies.

Parallel to advancements in segmentation models, the devel-

opment of large, annotated datasets revolutionized model training and evaluation. Addressing the persistent challenge of accurately segmenting both nuclei and whole cells across diverse cell types and imaging platforms, Greenwald et al. [69] introduced Mesmer, a deep learning-based segmentation model, in 2022. Trained on TissueNet, a dataset containing over 1.3 million whole-cell and nuclear annotations from nine tissue types and six imaging platforms, Mesmer achieved human-level performance in segmentation (Figure 6a). The architecture was based on a ResNet50 backbone coupled with an FPN, which utilizes dual input channels for precise segmentation. The model integrates its outputs with a watershed algorithm to generate detailed instance masks, overcoming limitations of prior approaches, such as nuclear expansion methods (Figure 6b–d). Mesmer's key innovation lies in its adaptability and scalability, supported by DeepCell, an open-source framework enabling both cloud-based and local deployment. Extensive benchmarking demonstrated that Mesmer outperformed earlier models, including StarDist [62,63] and Cellpose [66-68], when trained on similar datasets, while also being faster. Additionally, Mesmer showed robust generalization across unseen tissue types and imaging platforms, making it a versatile tool for large-scale imaging analyses. This combination of scalability and accuracy establishes Mesmer as a transformative solution for biological and clinical imaging workflows.

Despite these advancements, significant challenges remain. The diversity of cell types and imaging modalities continues to test the generalization capabilities of existing models. While approaches like StarDist [62,63] prioritize geometric precision and Cellpose [66-68] emphasizes robustness and usability, future research must address the integration of multimodal data, real-time segmentation, and lightweight architectures suitable for deployment in clinical settings. Meanwhile, transformer-based architectures, including SwinUNet [72] and TransUNet [73], leverage self-attention mechanisms to overcome the limitations of CNNs in modeling long-range dependencies and global context. In 2023, Chen et al. [70] proposed SCS, a transformer-based model that fuses high-resolution spatial transcriptomics and imaging data, enabling accurate cell segmentation and spot-to-cell assignment in challenging subcellular-resolution spatial transcriptomics datasets. Furthermore, large foundational models such as the SAM [47,48], which utilizes extensive pre-training and prompt-driven segmentation strategies, provide promising capabilities in zero-shot and few-shot segmentation. Additionally, semi- and self-supervised learning techniques show great potential for reducing the reliance on large, annotated datasets, paving the way for more scalable and efficient cell segmentation solutions [74-76].

4. Discussion and outlook

The convergence of live-cell imaging and adaptive segmentation

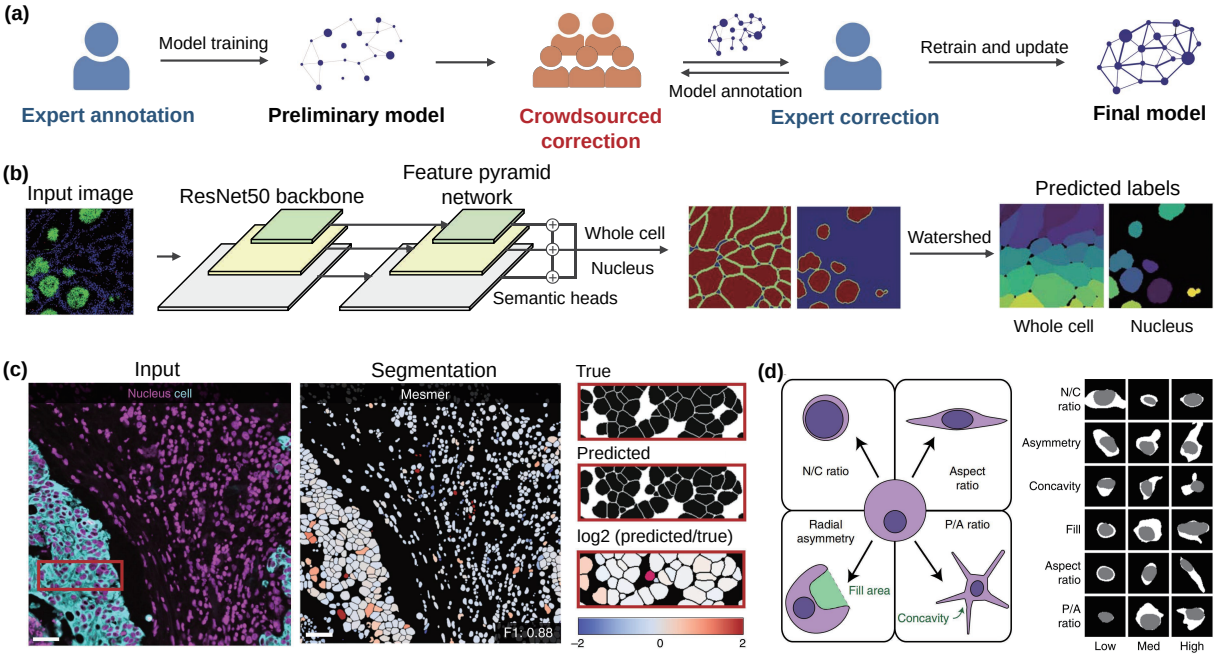


Figure 6 Mesmer achieves human-level performance in whole-cell and nuclear segmentation. **a.** Workflow of the Mesmer approach. Annotations are created from scratch to train an initial model. Next, new data are processed through the model to generate predictions, which serve as a baseline for correction by annotators. As corrected annotations are added to the dataset, the model iteratively improves, reducing errors and accelerating subsequent annotation. Finally, the refined model can accurately segment new images without human intervention. **b.** Images are fed into a ResNet50 backbone integrated with a FPA. Two semantic heads are employed to produce pixel-level predictions. The first head classifies each pixel as part of the interior, border, or background of a cell. The second head identifies the center of each cell to facilitate segmentation. **c.** A color overlay of a representative colorectal carcinoma image highlights the segmentation results. The inset compares ground truth with predicted labels from a small region and visualizes segmentation accuracy. **d.** Morphological metrics for cell shape analysis. A schematic demonstrates automated cell shape parameter extraction, including metrics such as the nuclear-to-cytoplasm (N/C) ratio, aspect ratio, concavity, radial asymmetry, and perimeter-to-area (P/A) ratio. Predicted segmentations categorize cells along a spectrum from low to high for each morphological metric, enabling quantitative analysis of cellular phenotypes.

frameworks has ushered in a new era of cellular deconstruction by enabling high-resolution, time-resolved analysis of biological processes [10]. When coupled with deep learning-driven segmentation algorithms, these datasets allow quantitative tracking of morphological variations, detection of phenotypic heterogeneity under perturbations, and mapping of signaling molecule localization with nanoscale precision [23,77]. By autonomously learning hierarchical features from complex, noisy datasets, these models bypass the need for predefined rules, offering scalable solutions for tasks ranging from single-cell tracking to segmentation of cell-dense regions, and address critical limitations of classical methods [78].

Recent advances in super-resolution techniques such as stimulated emission depletion (STED) [79], structured illumination microscopy (SIM) [80], and photoactivated localization microscopy (PALM) [81] have surpassed the diffraction limit, facilitating nanoscale analysis of cellular features. However, these systems introduce increased data heterogeneity, lower SNR, and greater computational demands [14]. Furthermore, the proliferation of 3D imaging and multi-modal datasets has amplified these challenges, requiring algorithms to adapt to anisotropic resolution and variable image quality [51]. Thus, the choice of microscopy modality and acquisition parameters not only determines the granularity and type of biological information available but also shapes the annotation workload, preprocessing needs, and achievable segmentation accuracy and generalizability [54,82]. Recognizing these distinctions is crucial for the development and benchmarking of robust, adaptable segmentation frameworks across diverse experimental conditions.

The development of robust segmentation frameworks continues to face two fundamental requirements: generalizability across diverse biological contexts and maintenance of high throughput capabilities. Cellular morphologies and structures often exhibit intricate features that vary significantly in size, shape, and fluorescence intensity depending on experimental conditions, labeling strategies, and the optical properties of the imaging system [52]. Notably, the inherent dynamism of living cellular systems, such as the cell membrane and flowing cytoplasm, introduces unique computational obstacles when analyzing time-dependent morphological transformations [83]. Addressing these challenges requires not only algorithmic improvements and architectural innovations but also systematic integration of optical imaging optimizations, physics-aware preprocessing, and standardized dataset curation. By bridging computational models with experimental realities through such multidimensional optimization, next-generation segmentation tools could achieve unprecedented adaptability without compromising processing efficiency [84].

3D imaging offers unparalleled capabilities in capturing spatial and dynamic features of cellular systems, yet imposes significant computational and analytical burdens. Challenges such as anisotropic resolution, signal attenuation, and structural overlap compound segmentation complexity exacerbate the scarcity of high-quality annotated datasets [85]. Emerging solutions are focusing on cross-modality data fusion to mitigate resolution discrepancies and self-supervised learning frameworks to leverage temporal consistency in dynamic imaging sequences [53,75]. Integrating physics-informed constraints, such as optical scattering models and biomechanical properties, will enhance segmentation fidelity under biologically realistic conditions [86]. Concurrent development of automated configuration capabilities and distributed edge computing frameworks could dramatically optimize processing efficiency [87]. These innovations will transform multidimensional imaging data from mere visualization tools into quantitative engines for mechanistic biology, supporting real-time interrogation of cellular dynamics and robust analysis of large-scale volumetric datasets.

The transition from technical capability to biological utility hinges on implementing user-friendly design principles. Next-generation tools should prioritize such key features: intelligent workflow automation that reduces manual preprocessing, minimizes manual intervention, and enables researchers with limited computational expertise to harness deep learning effectively [84]. A particularly promising direction involves collaborative annotation platforms where biologists can intuitively correct model outputs through human-in-the-loop feedback, teaching algorithms to "see" through expert eyes [68]. The heterogeneity in the morphology of different types of cells and the dynamic complexity of biological processes further necessitate customized analysis, where adaptive models integrate domain-specific priors to address context-dependent segmentation challenges [88].

Organelle segmentation is increasingly vital in live-cell imaging. Unlike cells or nuclei, organelles are much smaller, exhibit more complex and variable shapes, and often fall below the optical resolution limit [89-91]. Conventional segmentation methods struggle to resolve these features, and even deep learning approaches require specialized designs and high-quality datasets. In 2021, Sekh et al. [92] developed a physics-based simulation-supervised framework enabling robust segmentation of mitochondria and vesicles in noisy or low-resolution images. In the same year, Lefebvre et al. [93] introduced Mitometer, an algorithm for segmentation and tracking of mitochondria in live-cell time-lapse images. Recently, we developed MoDL, a deep learning framework that enables precise mitochondrial segmentation and morphological analysis for function prediction [94]. Future progress will depend on multi-scale integration, dynamic tracking, and reducing annotation requirements to advance robust, generalizable organelle analysis [95].

In conclusion, a synergistic combination of image segmentation and deep learning has recently achieved significant success in live-cell imaging. Deep learning has already proven invaluable for both enhancing the performance of segmentation methods and providing a way to efficiently interpret increasingly complex image analysis. These data-driven methods also have promising potential to reduce time and resource demands, leading to the broadening utility of image segmentation in life sciences.

Authors' contributions Bo Peng and Lin Li: Conceptualization. Zhijun Tan: Literature search and data curation. Zhijun Tan and Yang Ding: Writing – original draft. Yang Ding, Jintao Li, and Bin Fang: Writing – review & editing. Zhijun Tan and Yang Ding: Visualization. Lin Li, Bo Peng, and Hua Bai: Supervision. Bo Peng and Lin Li: Funding acquisition. All authors have read and agreed to the published version of the manuscript.

Compliance and ethics The author(s) declare that they have no conflict of interest.

Funding This work was supported by the National Natural Science Foundation of China (62475216, 22577108), Fundamental and

Interdisciplinary Disciplines Breakthrough Plan of the Ministry of Education of China (JYB2025XDXM406), Key Research and Development Program of Shaanxi (2024GH-ZDXM-37), Fujian Provincial Natural Science Foundation of China (2024J01060), Xiamen Science and Technology Program (3502Z20254028), State Key Laboratory of Vaccines for Infectious Diseases, Xiang An Biomedicine Laboratory (2024XAKJ0103005), Innovation Foundation for Doctorate Dissertation of Northwestern Polytechnical University (CX2023098), Startup Program of XMU, and Fundamental Research Funds for the Central Universities.

References

1. Peng H, Zhao M, Liu X, Tong T, Zhang W, Gong C, et al. Biomimetic materials to fabricate artificial cells. Chem Rev. 2024; 124: 13178–215.
2. Li N, Zhang W, Li Y, Lin JM. Analysis of cellular biomolecules and behaviors using microfluidic chip and fluorescence method. Trac Trends Anal Chem. 2019; 117: 200–14.
3. Seal S, Trapotsi MA, Spjuth O, Singh S, Carreras-Puigvert J, Greene N, et al. Cell Painting: A decade of discovery and innovation in cellular imaging. Nat Methods. 2025; 22: 254–68.
4. Chi H, Pepper M, Thomas PG. Principles and therapeutic applications of adaptive immunity. Cell. 2024; 187: 2052–78.
5. Xu CS, Pang S, Shtengel G, Müller A, Ritter AT, Hoffman HK, et al. An open-access volume electron microscopy atlas of whole cells and tissues. Nature. 2021; 599: 147–51.
6. Torkamani A, Andersen KG, Steinhubl SR, Topol EJ. High-definition medicine. Cell. 2017; 170: 828–43.
7. Xu C, Nedergaard M, Fowell DJ, Friedl P, Ji N. Multiphoton fluorescence microscopy for *in vivo* imaging. Cell. 2024; 187: 4458–87.
8. Kubota R, Tanaka W, Hamachi I. Microscopic imaging techniques for molecular assemblies: Electron, atomic force, and confocal microscopies. Chem Rev. 2021; 121: 14281–347.
9. Schwartz M, Israel U, Wang XJ, Laubscher E, Yu C, Dilip R, et al. Scaling biological discovery at the interface of deep learning and cellular imaging. Nat Methods. 2023; 20: 956–7.
10. Shroff H, Testa I, Jug F, Manley S. Live-cell imaging powered by computation. Nat Rev Mol Cell Biol. 2024; 25: 443–63.
11. Alieva M, Wezenaar AKL, Wehrens EJ, Rios AC. Bridging live-cell imaging and next-generation cancer treatment. Nat Rev Cancer. 2023; 23: 731–45.
12. Grimm, JB, English BP, Chen J, Slaughter JP, Zhang Z, Revyakin A, et al. A general method to improve fluorophores for live-cell and single-molecule microscopy. Nat Methods. 2015; 12: 244–50.
13. Bishop A. Live cell imaging of signaling networks using a conventional microscope. Nat Biotechnol. 2024; 42: 31.
14. Torrado B, Pannunzio B, Malacrida L, Digman MA. Fluorescence lifetime imaging microscopy. Nat Rev Meth Primers. 2024; 4: 80.
15. Huo L, Jiao JL, Chen L, Yu Z, Hutvagner G, Li J. Single-cell multi-omics sequencing: Application trends, COVID-19, data analysis issues and prospects. Brief Bioinform. 2021; 22: bbab229.
16. Song J, Liu Y, Zhang X, Wu Q, Gao J, Wang W, et al. Entropy subspace separation-based clustering for noise reduction (ENCORE) of scRNA-seq data. Nucleic Acids Res. 2021; 49: e18.
17. Driouchi A, Bretan M, Davis BJ, Heckert A, Seeger M, Silva MB, et al. Oblique line scan illumination enables expansive, accurate and sensitive single-protein measurements in solution and in living cells. Nat Methods. 2025; 22: 559–68.
18. Nketia TA, Sailem H, Rohde G, Machiraju R, Rittscher J. Analysis of live cell images: Methods, tools and opportunities. Methods. 2017; 115: 65–79.
19. Otsu N. A threshold selection method from gray-level histograms. IEEE Trans Syst Man Cybern. 1979; 9: 62–6.
20. Vincent L, Soille P. Watersheds in digital spaces: An efficient algorithm based on immersion simulations. IEEE Trans Pattern Anal Mach Intell. 1991; 13: 583–98.
21. Wang H, Rivenson Y, Jin Y, Wei Z, Gao R, Günaydın H, et al. Deep learning enables cross-modality super-resolution in fluorescence microscopy. Nat Methods. 2019; 16: 103–10.
22. Kaseva T, Omidali B, Hippeläinen E, Mäkelä T, Wilppu U, Sofiev A, et al. Marker-controlled watershed with deep edge emphasis and optimized H-minima transform for automatic segmentation of densely cultivated 3D cell nuclei. BMC Bioinform. 2022; 23: 289.
23. Pylvänäinen JW, Gómez-de-Mariscal E, Henriques R, Jacquemet G. Live-cell imaging in the deep learning era. Curr Opin Cell Biol. 2023; 85: 102271.
24. Ma Q, Xu D. Deep learning shapes single-cell data analysis. Nat Rev Mol Cell Biol. 2022; 23: 303–4.
25. Derry A, Krzywinski M, Altman N. Convolutional neural networks. Nat Methods. 2023; 20: 1269–70.
26. Hu C, He S, Lee YJ, He Y, Kong EM, Li H, et al. Live-dead assay on unlabeled cells using phase imaging with computational specificity. Nat Commun. 2022; 13: 713.
27. Szabó G, Bonaiuti P, Ciliberto A, Horváth A. Enhancing cell tracking with a time-symmetric deep learning approach. npj Syst Biol Appl. 2025; 11: 25.
28. Robitaille MC, Byers JM, Christodoulides JA, Raphael MP. Self-supervised machine learning for live cell imagery segmentation. Commun Biol. 2022; 5: 1162.
29. Liu Y, Jin Y, Azizi E, Blumberg AJ. Cellstitch: 3D cellular anisotropic image segmentation via optimal transport. BMC Bioinformatics. 2023; 24: 480.
30. Wu L, Chen A, Salama P, Winfree S, Dunn KW, Delp EJ. NISNet3D: Three-dimensional nuclear synthesis and instance segmentation for fluorescence microscopy images. Sci Rep. 2023; 13: 9533.
31. González-Díaz I, Baz-Hormigos CE, Díaz-de-María F. A generative model for concurrent image retrieval and ROI segmentation. IEEE Trans Multimed. 2014; 16: 169–83.
32. Araújo FHD, Silva RRV, Ushizima DM, Rezende MT, Carneiro CM, Campos Bianchi AG, et al. Deep learning for cell image segmentation and ranking. Comput Med Imag Graph. 2019; 72: 13–21.
33. Strack R. Deep learning in imaging. Nat Methods. 2019; 16: 17.
34. Hesamian MH, Jia W, He X, Kennedy P. Deep learning techniques for medical image segmentation: Achievements and challenges. J Digit Imaging. 2019; 32: 582–96.
35. Yang R, Yu Y. Artificial convolutional neural network in object detection and semantic segmentation for medical imaging analysis. Front Oncol. 2021; 11: 638182.
36. Goh TY, Basah SN, Yazid H, Aziz Safar MJ, Ahmad Saad FS. Performance analysis of image thresholding: Otsu technique. Measurement. 2018; 114: 298–307.
37. Tareef A, Song Y, Huang H, Feng D, Chen M, Wang Y, et al. Multi-pass fast watershed for accurate segmentation of overlapping cervical cells. IEEE Trans Med Imaging. 2018; 37: 2044–59.
38. Wang JX, Zhao S, Liu Z, Tian Y, Duan F, Pan Y. An active contour model based on adaptive threshold for extraction of cerebral vascular structures. Comput Math Methods Med. 2016; 2016: 6472397.
39. Ma DD, Liao Q, Chen Z, Liao R, Ma H. Adaptive local-fitting-based active contour model for medical image segmentation. Signal Process Image Commun. 2019; 76: 201–13.
40. Hajdowska K, Student S, Borys D. Graph based method for cell segmentation and detection in live-cell fluorescence microscope imaging. Biomed Signal Process Control. 2022; 71: 103071.
41. Shelhamer E, Long J, Darrell T. Fully convolutional networks for semantic segmentation. IEEE Trans Pattern Anal Mach Intell. 2017; 39: 640–51.
42. Azad R, Aghdam EK, Rauland A, Jia Y, Avval AH, Bozorgpour A, et al. Medical image segmentation review: The success of U-Net. IEEE Trans Pattern Anal Mach Intell. 2024; 46: 10076–95.
43. He K, Gkioxari G, Dollar P, Girshick R. Mask R-CNN. IEEE Trans Pattern Anal Mach Intell. 2020; 42: 386–97.
44. He K, Zhang X, Ren S, Sun J. Deep residual learning for image recognition. In: 2016 IEEE Conference on Computer Vision and Pattern Recognition (CVPR). Las Vegas: IEEE; 2016: 770–8.
45. Hörst F, Rempe M, Heine L, Seibold C, Keyl J, Baldini G, et al. CellViT: Vision Transformers for precise cell segmentation and classification. Med Image Anal. 2024; 94: 103143.
46. Zhang X, Lin Z, Wang L, Chu YS, Yang Y, Xiao X, et al. SwinCell: A 3D transformer and flow-based framework for improved cell segmentation. Commun Biol. 2025; 8: 962.
47. Kirillov A, Mintun E, Ravi N, Mao H, Rolland C, Gustafson L, et al. Segment anything. In: 2023 IEEE/CVF International Conference on Computer Vision (ICCV). Paris: IEEE; 2023: 4015–26.
48. Ma J, He Y, Li F, Han L, You C, Wang B. Segment anything in medical images. Nat Commun. 2024; 15: 654.
49. Ziółko B, Emms D, Ziółko M. Fuzzy evaluations of image segmentations. IEEE Trans Fuzzy Syst. 2018; 26: 1789–99.
50. Thisanke H, Deshan C, Chamith K, Seneviratne S, Vidanaarachchi R, Herath D. Semantic segmentation using Vision Transformers: A survey. Eng Appl Artif Intell. 2023; 126: 106669.
51. Al Garea S, Das S. Image segmentation methods: Overview, challenges, and future directions. In: 2024 Seventh International Women in Data Science Conference at Prince Sultan University (WiDS PSU). Riyadh: IEEE; 2024: 56–61.
52. Maška M, Ulman V, Delgado-Rodriguez P, Gómez-de-Mariscal E, Nečasová T, Guerrero Peña FA, et al. The cell tracking challenge: 10 years of objective benchmarking. Nat Methods. 2023; 20: 1010–20.
53. Geuenich MJ, Gong DW, Campbell KR. The impacts of active and self-supervised learning on efficient annotation of single-cell expression data. Nat Commun. 2024; 15: 1014.
54. Park J, Bai B, Ryu D, Liu T, Lee C, Luo Y, et al. Artificial intelligence-enabled quantitative phase imaging methods for life sciences. Nat Methods. 2023; 20: 1645–60.
55. Moen E, Bannon D, Kudo T, Graf W, Covert M, Van Valen D. Deep learning for cellular image analysis. Nat Methods. 2019; 16: 1233–46.
56. Chen X, Zhou X, Wong STC. Automated segmentation, classification, and tracking of cancer cell nuclei in time-lapse microscopy. IEEE Trans Biomed Eng. 2006; 53: 762–6.
57. Ji X, Li Y, Cheng J, Yu Y, Wang M. Cell image segmentation based on an improved watershed algorithm. In: 8th International Congress on Image and

Signal Processing (CISP). Shenyang: IEEE; 2015: 433–7.
58. Abdolhoseini, M, Kluge MG, Walker FR, Johnson SJ. Segmentation of heavily clustered nuclei from histopathological images. Sci Rep. 2019; 9: 4551.
59. Niaz A, Iqbal E, Akram F, Kim J, Choi KN. Self-initialized active contours for microscopic cell image segmentation. Sci Rep. 2022; 12: 14947.
60. Fang Y, Zhong B. Cell segmentation in fluorescence microscopy images based on multi-scale histogram thresholding. Math Biosci Eng. 2023; 20: 16259–78.
61. Ronneberger O, Fischer P, Brox T. U-Net: Convolutional networks for biomedical image segmentation. In: Medical Image Computing and Computer-Assisted Intervention–MICCAI 2015. Munich: Springer; 2015: 234–41.
62. Schmidt U, Weigert M, Broaddus C, Myers G. Cell detection with star-convex polygons. In: Medical Image Computing and Computer Assisted Intervention–MICCAI 2018. Granada: Springer; 2018: 265–73.
63. Weigert M, Schmidt U, Haase R, Sugawara K, Myers G. Star-convex polyhedra for 3D object detection and segmentation in microscopy. In: 2020 IEEE Winter Conference on Applications of Computer Vision (WACV). Snowmass Village: IEEE; 2020: 3655–62.
64. Caicedo, JC, Goodman A, Karhohs KW, Cimini BA, Ackerman J, Haghighi M, et al. Nucleus segmentation across imaging experiments: The 2018 Data Science Bowl. Nat Methods. 2019; 16: 1247–53.
65. Falk T, Mai D, Bensch R, Çiçek Ö, Abdulkadir A, Marrakchi Y, et al. U-Net: Deep learning for cell counting, detection, and morphometry. Nat Methods. 2019; 16: 67–70.
66. Stringer C, Wang T, Michaelos M, Pachitariu, M. Cellpose: A generalist algorithm for cellular segmentation. Nat Methods. 2021; 18: 100–6.
67. Pachitariu M, Stringer C. Cellpose 2.0: How to train your own model. Nat Methods. 2022; 19: 1634–41.
68. Stringer C, Pachitariu M. Cellpose3: One-click image restoration for improved cellular segmentation. Nat Methods. 2025; 22: 592–9.
69. Greenwald NF, Miller G, Moen E, Kong A, Kagel A, Dougherty T, et al. Whole-cell segmentation of tissue images with human-level performance using large-scale data annotation and deep learning. Nat Biotechnol. 2022; 40: 555–65.
70. Chen H, Li D, Bar-Joseph Z. SCS: Cell segmentation for high-resolution spatial transcriptomics. Nat Methods. 2023; 20: 1237–43.
71. Kumar N, Verma R, Sharma S, Bhargava S, Vahadane A, Sethi A. A dataset and a technique for generalized nuclear segmentation for computational pathology. IEEE Trans Med Imaging. 2017; 36: 1550–60.
72. Cao H, Wang Y, Chen J, Jiang D, Zhang X, Tian Q, et al. Swin-unet: Unet-like pure transformer for medical image segmentation. In: Computer Vision–ECCV 2022 Workshops. Tel Aviv: Springer; 2023: 205–18.
73. Chen JN, Mei J, Li X, Lu Y, Yu Q, Wei Q, et al. TransUNet: Rethinking the U-Net architecture design for medical image segmentation through the lens of transformers. Med Image Anal. 2024; 97: 103280.
74. Shrestha P, Kuang N, Yu J. Efficient end-to-end learning for cell segmentation with machine generated weak annotations. Commun Biol. 2023; 6: 232.
75. van Engelen JE, Hoos HH. A survey on semi-supervised learning. Mach Learn. 2020; 109: 373–440.
76. Zong Y, Mac Aodha O, Hospedales TM. Self-supervised multimodal learning: A survey. IEEE Trans Pattern Anal Mach Intell. 2025; 47: 5299–318.
77. Dong Y, Qi L, Zhao F, Chen Y, Liang L, Wang J, et al. Uncovering dynamic transcriptional regulation of methanogenesis via single-cell imaging of archaeal gene expression. Nat Commun. 2025; 16: 2255.
78. Zhao S, Chen DP, Fu T, Yang JC, Ma D, Zhu XZ, et al. Single-cell morphological and topological atlas reveals the ecosystem diversity of human breast cancer. Nat Commun. 2023; 14: 6796.
79. Vicidomini G, Bianchini P, Diaspro A. STED super-resolved microscopy. Nat Methods. 2018; 15: 173–82.
80. Chen X, Zhong S, Hou Y, Cao R, Wang W, Li D, et al. Superresolution structured illumination microscopy reconstruction algorithms: A review. Light Sci Appl. 2023; 12: 172.
81. Lelek M, Gyparaki MT, Beliu G, Schueder F, Griffié J, Manley S, et al. Single-molecule localization microscopy. Nat Rev Meth Primers. 2021; 1: 39.
82. Hollandi R, Szkalisity A, Toth T, Tasnadi E, Molnar C, Mathe B, et al. nucleAIzer: A parameter-free deep learning framework for nucleus segmentation using image style transfer. Cell Syst. 2020; 10: 453–8.
83. Adhyapak P, Kapoor S. Membrane dynamics in health and disease: Impact on cellular signalling. J Membr Biol. 2019; 252: 213–26.
84. Ma J, Xie R, Ayyadhury S, Ge C, Gupta A, Gupta R, et al. The multimodality cell segmentation challenge: Toward universal solutions. Nat Methods. 2024; 21: 1103–13.
85. Goceri E. Challenges and recent solutions for image segmentation in the era of deep learning. In: 2019 Ninth International Conference on Image Processing Theory, Tools and Applications (IPTA). Istanbul: IEEE; 2019: 1–6.
86. Xiang Y, Pan B, Luo L. A new model updating strategy with physics-based and data-driven models. Struct Multidiscip Optim. 2021; 64: 163–76.
87. Isensee F, Jaeger PF, Kohl SAA, Petersen J, Maier-Hein KH. nnU-Net: A self-configuring method for deep learning-based biomedical image segmentation. Nat Methods. 2021; 18: 203–11.
88. Panigrahi S, Murat D, Le Gall A, Martineau E, Goldlust K, Fiche JB, et al. Misic, a general deep learning-based method for the high-throughput cell segmentation of complex bacterial communities. Elife. 2021; 10: e65151.
89. Fischer CA, Besora-Casals L, Rolland SG, Haeussler S, Singh K, Duchen M, et al. MitoSegNet: Easy-to-use deep learning segmentation for analyzing mitochondrial morphology. iScience. 2020; 23: 101601.
90. Lu M, Christensen CN, Weber JM, Konno T, Läubli NF, Scherer KM, et al. ERnet: A tool for the semantic segmentation and quantitative analysis of endoplasmic reticulum topology. Nat Methods. 2023; 20: 569–79.
91. Huang J, Luo Y, Guo Y, Li W, Wang Z, Liu G, et al. Accurate segmentation of intracellular organelle networks using low-level features and topological self-similarity. Bioinformatics. 2024; 40: btae559.
92. Sekh AA, Opstad IS, Godtliebsen G, Birgisdottir ÅB, Ahluwalia BS, Agarwal K, et al. Physics-based machine learning for subcellular segmentation in living cells. Nat Mach Intell. 2021; 3: 1071–80.
93. Lefebvre AEYT, Ma D, Kessenbrock K, Lawson DA, Digman MA. Automated segmentation and tracking of mitochondria in live-cell time-lapse images. Nat Methods. 2021; 18: 1091–102.
94. Ding Y, Li J, Zhang J, Li P, Bai H, Fang B, et al. Mitochondrial segmentation and function prediction in live-cell images with deep learning. Nat Commun. 2025; 16: 743.
95. Cutler KJ, Stringer C, Lo TW, Rappez L, Stroustrup N, Brook Peterson S, et al. Omnipose: A high-precision morphology-independent solution for bacterial cell segmentation. Nat Methods. 2022; 19: 1438–48.